

DIVERSITY OF EXPLOSIVE VOLCANIC FEATURES IN SCHRÖDINGER BASIN ON THE MOON.

M.J.B. Henderson^{1,2,3} B.H.N. Horgan¹ and L.R. Gaddis⁴, ¹Purdue University, 610 Purdue Mall, West Lafayette, IN (marie@purdue.edu) ²Center for Space Sciences and Technology, University of Maryland, Baltimore County ³Solar System Exploration Division, NASA/GSFC, Greenbelt, MD 20771 ⁴Lunar and Planetary Institute.

Introduction: Schrödinger basin has been an area of heightened interest for lunar exploration due to the proximity of well-preserved impact and volcanic materials that could be accessed in a single mission. Schrödinger is a 320 km diameter Imbrium-aged impact crater located within South Pole-Aitken (SPA) basin on the lunar far side, centered at 138°E, 75°S [1]. The Pre-Nectarian-aged basin is slated as a landing site for two payload suites delivered by (CLPS Missions in 2024 [2].

The relationship between the volcanic deposits in Schrödinger is not well understood. A variety of origins have been hypothesized for the cone, flow, and other possibly related features in the basin. Here we use orbital reflectance spectroscopy to determine the mineralogy and crystallinity of the volcanic deposits and ultimately assess the basin's volcanic eruption history. This study aims to characterize the eruption style of volcanic deposits, both whether eruptions in the basin were explosive vs. effusive and the nature of any explosive eruptions. Understanding the eruption properties of the Schrödinger volcanics provides key insights into magma source regions in the lunar interior and will provide context for future missions.

Background: Visible wavelength images [3] reveal that the pyroclastic deposits within the Schrödinger basin may be relatively complex, with multiple pyroclastic deposits (Fig 1). In the LROC WAC mosaic, low albedo units within the inner-peak ring stand out as distinct from the basin floor. Figure 1 outlines and labels these units as the cone, lobate mafic, and ridge units.

The Clementine UVVIS instrument [4] provided the first spectral analysis of Schrödinger [5]. A single M³ image was then analyzed to test their Clementine results [6]. Previously the Schrödinger was examined with Level 1 M³ hyperspectral data [7,8], but the analysis was limited to material exposed by impacts. These studies examined the peak-ring, inner peak-ring floor, as well as the cone, lobate mafic, and ridge pyroclastic units.

Methods: An M³ mosaic of Schrödinger was constructed with bounds 110-155°E and 82-67°N in an orthographic projection with six spectral images (Fig 2), using the methods described in [9,10]. M³ observations of Schrödinger have a resolution of 280 m/pixel in 86 spectral channels [11] with data obtained in optical period 2C [12]. Because of these less ideal observation conditions, spectra extracted from M³ images in Schrödinger tend to exhibit significant noise.

Spectral diversity maps were created by parameterizing the 1- and 2-μm absorption bands in the

M³ mosaic. In this study, spectral variability was assessed using two types of spectral parameters: (1) spectral indices using simple arithmetic (e.g., Glass spectral parameter detects the wings of the glass iron absorption based on the average band depth below the continuum at 1.15, 1.18, and 1.20 μm.) and (2) 1 and 2 μm band position, area, and shape parameters derived from our continuum removed mosaic.

Results: We completed the first hyperspectral map of the Schrödinger basin with M³ data (Fig 1).

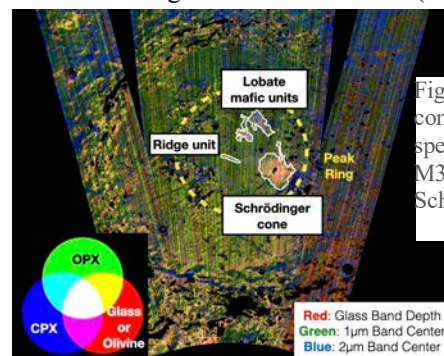


Figure 1: Mosaicked composite RGB spectral maps from M³ data of Schrödinger basin.

The volcanic deposits are spectrally distinct units. RGB composite images are shown in (Figs 1-2), which highlights the mineralogical diversity of Schrödinger. The subtle horizontal striping across the M³ frames in (Figs 1-2) maps is due to slight resolution and detector sensitivity changes. Analysis of these data reveals that the volcanic terrains of the cone and the inner-peak ring pyroclastic deposits are spectrally distinct from impact features as well as the inner-peak ring floor.

Spectra collected from Schrödinger are shown in Fig 3. The large conical edifice has bands centered near 0.98-1.10 and 1.85-2.00 μm and strong shoulders to long wavelengths on the 1 μm band, consistent with a mixture of glass and pyroxene and supporting an explosive origin (Fig 3) [9,13]. Olivine is unlikely to be a major contributor based on the band center positions, a 2 μm band, and the 1 μm band asymmetry.

The inner peak-ring lobate mafic unit exhibits bands near 0.95-1.05 μm and 1.8-2.0 μm, and the 1 μm band is narrow without any additional absorption that could be attributed to olivine or glass (Fig 3). Integrating the spectral map and the LROC imagery with the morphology of the lobate mafic unit leads to the first possible identification of small secondary vents or cones in Schrödinger (Fig 2e,f). Two C-shaped topographic rises resemble breached cones with diameters of 1.5 and 3.0 km and are consistent with detections in the glass parameter map (Fig 2f). Spectra of the cones (Fig 3) are

difficult to extract due to their size, but an average spectrum taken from both cones shows band centers near 1.03-1.05 μm and 1.80-1.90 μm , with a broad 1 μm band that may be consistent with glass.

The linear ridge unit is a thin lenticular unit isolated within the inner-peak ring basin (Fig 2c). The distinct linear ridge on the floor exhibit bands centered near 0.97 μm and 1.9-2.0 μm (Fig 3), attributed to the influence of CPX. The 1 μm band is wider than expected for CPX alone and exhibits additional absorption at long wavelengths, suggesting a contribution from glass.

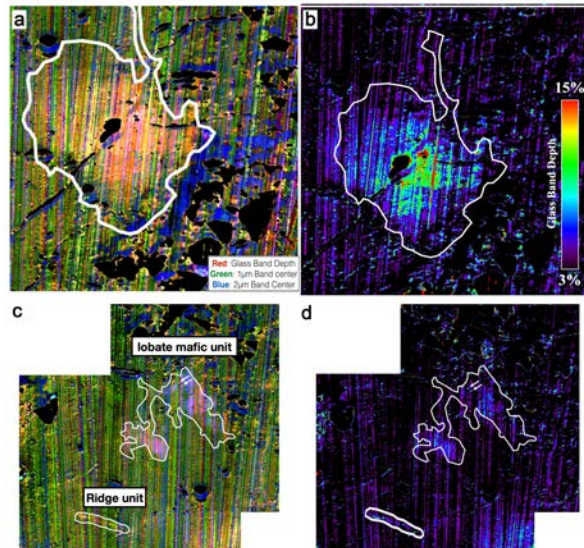


Figure 2: Subset of volcanic units within the inner-peak ring (a-b) focus on the pyroclastic cone (c-d) are focused on the lobate mafic and ridge units. (a,c) RGB spectral maps from M³ (c,f) Glass band depth parameter map. Arrows point to locations of potential volcanic cones.

Discussions: Schrödinger cone has spectral signatures consistent with a mixture of pyroxene and significant glass, indicating an explosive emplacement as previously theorized [7,14]. The spectral differences in the west and east sides of the volcanic vent (Fig 2b) can be attributed to the covering of the volcanic deposits by ejecta from more recent impacts.

The lobate mafic unit within the peak ring is spectrally distinct from the other volcanic units in Schrödinger. Previously, the lobate mafic unit was considered a mare unit that has erupted effusively instead of explosively [5–7]. However, we have also identified possible glass signatures on the flow associated with small edifices that appear to be small cinder cones. We hypothesize that the unit first erupted explosively, building an edifice like a terrestrial cinder cone, and then erupted the flow component to create the lobate morphology of the margins.

M³ spectra from the linear ridge could be attributed to the increased influence of CPX and potentially with a limited contribution from glass relative to the basin

floor. This detection corroborates the volcanic origin hypothesis because CPX and glass both likely represent juvenile magmatic material, similar to the lobate mafic unit. The presence of juvenile material with the location separated from the radial fractures leads us to believe that this was a magmatic intrusion that erupted through a fissure that created a thin layer of material that cooled quickly, overlaying the inner-peak ring floor.

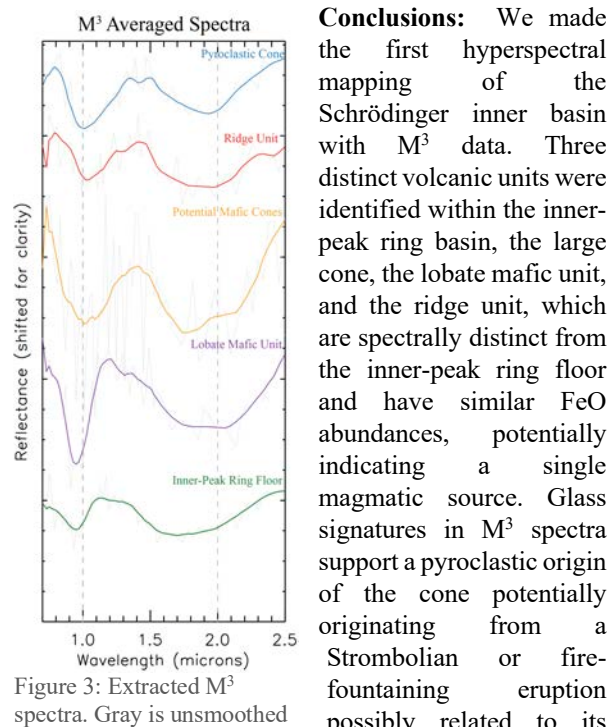


Figure 3: Extracted M³ spectra. Gray is unsmoothed possibly related to its location along the large radial graben. Smaller cones with potentially glassy spectral signatures have been identified within the lobate mafic units, suggesting an initial explosive pyroclastic eruption that later transitioned to an effusive component where coalesced pyroclasts flowed to create the lobed flow margins and a rough flow surface in radar images. The linear ridge unit exhibits spectra consistent with CPX and possible glass, which is unlike the basin floor but similar to the lobate mafic unit, thus confirming a volcanic origin over a tectonic feature.

Acknowledgments: We would like to thank David Mayer. This work was supported by the NSF GRFP (DGE-1333468) and in partnership with USGS Astro through NSF GRIP and supported in part by the NASA LDAP NNX17AC63G.

References: [1] Wilhelms et al., (1979), [2] NASA Artemis Plan, (2020), [3] Robinson et al., *SSR* (2010), [4] Nozette et al. 1994 [5] Shoemaker et al. *Science*. (1994), [6] Shankar et al. *Can. Jou. of Earth Sciences*. (2012). [7] Kramer et al. *Icarus* (2013) [8] Pieters et al. (2009), *Science*, [9] Horgan et al. *Icarus* (2014) [10] Bennett et al. *Icarus* (2016) [11] Pieters et al. *Curr. Sci* (2009) [12] Isaacson et al., *JGR Planets* (2013) [13] Cloutis et al. *Earth Moon and Planets* (1991) [14] Gaddis, L.R. et al. *Icarus* (2003).